THE SOLAR LIMB INTENSITY PROFILE

JOHN E. GAUSTAD AND JOHN B. ROGERSON, JR.
Princeton University Observatory, Princeton, New Jersey
Received April 12, 1961

ABSTRACT

A new determination of the intensity distribution of the solar limb at λ 5490 A has been made from a photograph taken by a balloon-borne telescope. The apparatus function for the telescope is derived from the data. This new determination supersedes that obtained from 1957 balloon-telescope photographs.

INTRODUCTION

In the summer of 1959, a 12-inch solar telescope was carried into the stratosphere by an unmanned balloon as part of the experiment known as Project Stratoscope. A description of the instrument and a discussion of other aspects of the experiment are given elsewhere (Bahng and Schwarzschild 1961; Danielson 1961; Rogerson 1961). This paper is concerned with the determination of the intensity profile of the extreme solar limb from a high-quality photograph obtained with this telescope. The method used follows closely that employed previously by one of the authors (Rogerson 1959). This new determination, however, is based on better observational material and hence supersedes the former one.

OBSERVATIONS AND MEASUREMENTS

Four exposures of extremely high quality were selected by visual inspection from over 60 good photographs of the solar limb. Microdensitometer tracings perpendicular to the limb were made on these exposures and compared. Little difference in the sharpness of the limb was found among these four, and so the one containing the longest traceable solar radius was selected for analysis (Fig. 1).

This exposure bears the Princeton designation 1959–D77. It was taken at 15:21 U.T. on September 24, 1959, at a point on the sun approximately 25° south of the equator on the western limb. The emulsion was Eastman Kodak Background X, which, with Wratten No. 99 and Corning No. 3384 filters, gives an effective wave length of 5490 A. This emulsion with its good sensitivity and moderate contrast was chosen especially for the study of the limb and sunspot umbrae. The scale on the film is 0.30 mm = 1 second of arc.

Three independent microdensitometer tracings along different solar radii were made with a slit of dimensions 3μ by 2000μ (0.01 by 7 seconds of arc) with the longer dimension positioned parallel to the limb. These dimensions are small enough that the smearing effect of the slit is completely negligible. Smooth curves were drawn through each tracing to eliminate the fluctuations caused by photographic grains, and values of the film transmission were read at a convenient interval of 0.05 mm (0.167 second of arc). This choice of interval is consistant with the theorem of information theory stating that the observed intensity function obtained with an instrument of finite aperture is completely specified by its values at the interval $\lambda/2d$, where d is the diameter of the aperture (Bracewell and Roberts 1954).

Calibration was carried out in the manner described by Rogerson (1959) with the aid of neutral density filters of measured transmission located near the edge of each frame. Frame D75, covering a region slightly inside the limb, was selected for this purpose. Tracings made across the filters gave measurements of the density on each

side of the eight filter edges and hence determined eight pairs of points on a calibration-curve. These points did not carry the curve to sufficiently low intensities, and so another frame, D80, upon which the limb crossed one filter edge at a large angle, was selected for additional measurements. Tracings were made across this filter edge parallel to and outside of the limb at regularly spaced intervals. By making use of the scattered light outside the limb, this procedure gave eight additional pairs of points on the low-intensity portion of the calibration-curve. The sixteen pairs of points were individually shifted along the log intensity axis until they all fitted onto a smooth curve.

This calibration-curve was then used to transform each of the three limb tracings from a density scale onto an intensity scale. These were averaged point by point, and a fourth smooth curve was drawn. The average standard deviation of the three tracings from this mean curve is about 4 per cent outside the limb (with a range of 1–9 per cent) and 1.6 per cent inside the limb (with a range of 0.8–3 per cent).

None of the three tracings reached zero intensity, even at a distance of several seconds outside the limb. Inspection showed, however, that they approached asymptotically an intensity 0.0064 times the intensity at the center of the solar disk. This constant background, attributed to uniform scattered light, was subtracted from all readings. The final observed profile, expressed in terms of the central disk intensity, is tabulated in Table 2.

THE APPARATUS FUNCTION

The observed limb profile $O(x)$ is the convolution of the true limb profile $T(x)$ with the apparatus function $A(x)$ according to the equation

$$O(x) = \int_{-\infty}^{\infty} A(x')T(x - x')\,dx' . \tag{1}$$

For purposes of computation, this can be approximated by

$$O_i = \sum_{j=-k}^{k} A_j T_{i-j} , \tag{2}$$

where $2k + 1$ is the number of non-zero points in the apparatus function.

We can consider these equations from two points of view. First, if we assume that $A(x)$ is known, we can solve for $T(x)$ by successive approximations. This is what we shall finally do to determine the true intensity profile inside the limb. However, from the other point of view, if we have some knowledge of $T(x)$, we can use equation (2) to obtain an estimate of $A(x)$. Eclipse measurements (Kristenson 1951) show that beyond the inflection point on the limb the intensity falls rapidly to zero. Hence any observed intensity beyond this point must come entirely from the effects of the apparatus function in smoothing out this sharp profile. We can use this fact to determine the wings of our apparatus function, then fit these wings to a core appropriate for a 12-inch aperture, and finally use the combined apparatus function to solve for the true intensity profile inside the limb. If we use the observed intensity profile outside the limb to determine part of the apparatus function, we cannot, of course, say anything about the true intensity profile in this region. Rogerson was unable to apply this method in his earlier analysis (Rogerson 1959) because the high threshold of the emulsion used made the faint extensions of the limb unobservable.

Let us then assume, on the basis of the eclipse observations, that the true limb intensity drops abruptly to zero at a certain point, i.e., that $T_i = 0$ for $i < k + 1$. Then equation (2) becomes, for $i < 2k + 1$,

$$O_i = \sum_{j=-k}^{i-k-1} A_j T_{i-j} . \tag{3}$$

If we solve this equation for the A with the largest subscript we obtain

$$A_{i-k-1} = \frac{O_i - \sum_{j=-k}^{i-k-2} A_j T_{i-j}}{T_{k+1}} . \tag{4}$$

If we now assume some approximate true limb profile T, we can use equation (4) to compute the apparatus function point by point, starting with its first non-zero value, which corresponds to the point on the observed curve O farthest from the limb.

As long as A remains small, as it does in the wings of the apparatus function, even comparatively large errors in the assumed true function T will lead to only small absolute errors in A. Thus the exact shape of the assumed approximation to the true limb is not important for this determination. This fact was borne out experimentally by trying different assumed true limb profiles in equation (4) and comparing the functions A obtained. One extreme assumption involved a true function T which was a straight line tangent to the observed profile 15 seconds of arc from the limb and which dropped to zero abruptly at the limb itself. Another trial function was obtained by combining Dunn's true limb profile (Dunn 1959) with the results of Kristenson's 1954 eclipse measurements (Kristenson 1960). The wings of the apparatus function obtained on the basis of these two assumptions are shown in Figure 2. They are identical in to $\frac{2}{3}$ second of arc from the peak, but, within this range, that obtained from the more correct assumption of the Dunn-Kristenson limb has lower values.

This then determines the wings of the apparatus function. We now assume that the core of the apparatus function will have the same shape as the theoretical diffraction pattern for a 12-inch aperture. We fit this theoretical core to the derived wing to obtain the complete apparatus function, but first we reduce the core by a scale factor so that the integral of the combined function remains equal to unity. The fitting is done at a point about $\frac{1}{3}$ second of arc from the peak, as shown in Figure 2, with the wing derived from the Dunn-Kristenson true profile being taken as the best value in the range beyond $\frac{1}{3}$ second of arc. This combined apparatus function—theoretical core and observed wing—is shown in Figure 2 and tabulated in Table 1.

We may now ask the question of how much light is scattered out of the primary image by the wings of the apparatus function. In the case of the limb measurements, we are primarily interested in the line apparatus function given in Figure 2 and Table 1; but, in a general discussion of the performance of the instrument and in other applications such as the measurement of the brightness fluctuation of the granulation, we would want to consider the point apparatus function instead. We shall discuss both cases.

If we define the scattered fraction $S(r_0)$ as the fraction of light in an image which is scattered beyond a distance r_0, then, for the line apparatus function $A(x)$,

$$S_L(r_0) = 2\int_{r_0}^{\infty} A(x)\,dx . \tag{5}$$

We choose r_0 to be $\frac{1}{3}$ second of arc, the point where we fitted the theoretical core to the observed wings. Then a simple numerical integration gives

$$S_L(\tfrac{1}{3}'') = 0.24 . \tag{6}$$

We now consider the fraction of light scattered beyond a certain radius for the point apparatus function. The required relation with the line apparatus function is

$$S_p(r_0) = \int_{r_0}^{\infty} W(r)\,2\pi r\,dr = 2\int_{r_0}^{\infty} \frac{A(x)\,x\,dx}{(x^2 - r_0^2)^{1/2}}, \tag{7}$$

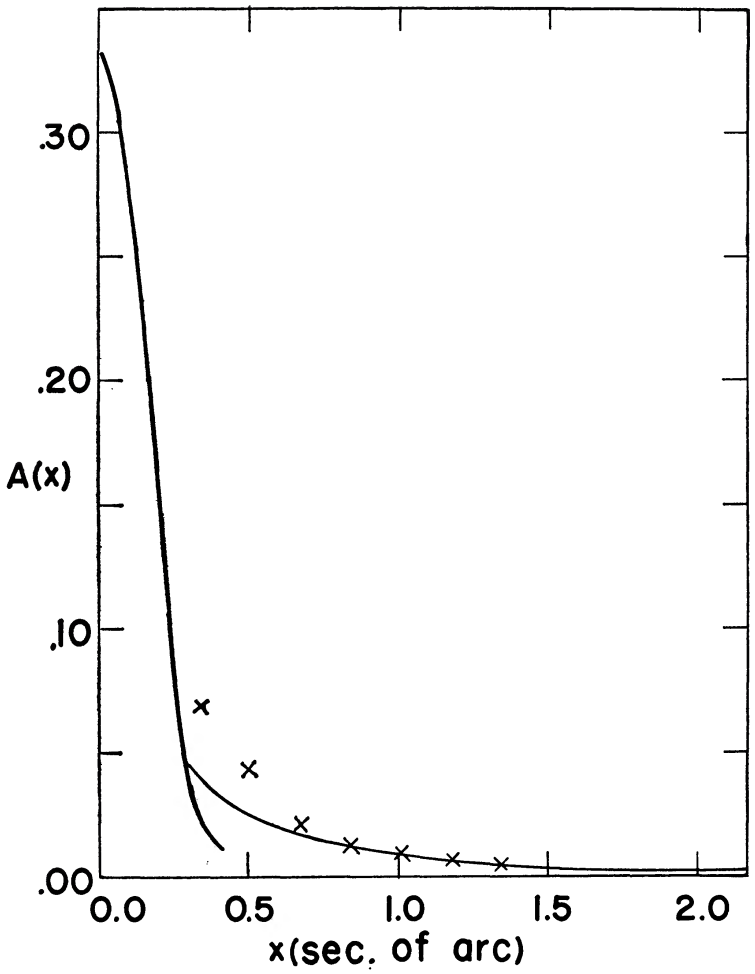

FIG. 2.—Apparatus function: theoretical line diffraction pattern (*heavy line*); observed wing obtained from Dunn-Kristenson assumed true limb profile (*light line*); observed wing obtained from straight line profile (*crosses*).

TABLE 1

APPARATUS FUNCTION

x (seconds of arc)	$A(x)$*	x (seconds of arc)	$A(x)$*	x (seconds of arc)	$A(x)$*
0 00	0 3365†	1 67..	0 0030	3 33....	0 0007
0 17 .	1900†	1 83 .	0023	4 00 .	0006
0.33..	.0386	2 00	0019	4 67..	0005
0 50..	0247	2.17.. ..	.0016	5 33 .	0004
0 67 .	0172	2 33..	0013	6 00...	.0003
0 83...	.0123	2 50 .	0011	6 67...	.0002
1 00 ...	0088	2 67...	0010	7 33 ..	0002
1 17 .	0063	2 83.....	0009	8 00 ...	.0001
1 33 ..	0049	3 00	0008	8 67.....	0001
1 50 . .	0 0038	3 17..... ..	0 0008	9.33...	0 0000

* Ordinates normalized for use in eq (2).

† Theoretical core of the line diffraction pattern for 12-inch aperture

where $W(r)$ is the point apparatus function. Again taking $r_0 = \frac{1}{3}$ second of arc, we find, by numerical integration, that

$$S_p(\tfrac{1}{3}'') = 0.35 \,. \tag{8}$$

If we now also take into account the constant background of scattered light discussed in the previous section, we find that the total contribution to the intensity at any point from scattered light, i.e., from light scattered from points $\frac{1}{3}$ second of arc or more away, is about 36 per cent. The theoretical value for the diffraction pattern of a 12-inch aperture is 19 per cent.

This value for the scattered light seems rather high. However, over 70 per cent of this is still within a radius of 1 second of arc and in most astronomical applications would still be considered to be in the primary image. The remaining 30 per cent is of such low intensity as to remain undetectable in most cases. We suspect that this phenomenon is fairly common in astronomical instruments, but it is only in dealing with measurements of such high resolution as that obtained with a balloon-borne telescope that such scattered light becomes of interest.

Finally, we compute the contrast transmission function for our instrument, that is, the Fourier transform of the apparatus function:

$$T(k) = 2\int_0^\infty A(x)\cos kx dx \,. \tag{9}$$

TABLE 2

OBSERVED AND TRUE LIMB PROFILES EXPRESSED IN TERMS OF INTENSITY AT DISK CENTER

Limb Distance (seconds of arc)	cos θ	I_{obs}	I_{true}	Limb Distance (seconds of arc)	cos θ	I_{obs}	I_{true}
+10 00		0 0000		−1 83	0 062	0 334	0 341
+ 9 17.		0004		2 00	064	338	345
+ 8 33		0007		2 17	067	341	347
+ 7 50		0010		2 33	069	345	350
+ 6 67		0014		2 50	072	348	354
+ 5 83		0017		2 67	074	350	355
+ 5 00		0023		2 83	077	352	356
+ 4 17		0030		3 00	079	353	358
+ 3 33		0041		3 17	081	355	359
+ 2 50		0054		3 33	083	356	360
+ 1 67		0043		4 17	093	363	365
+ 1 50		0106		5 00	102	369	371
+ 1 33		0124		5 83	110	375	376
+ 1 17		0150		6 67	117	381	381
+ 1 00		0187		7 50	124	387	387
+ 0 83		023		8 33	131	392	392
+ 0 67		031	0 004	9 17	137	398	398
+ 0 50		046	011	10 00	144	403	.403
+ 0 33		069	041	10 83	150	408	408
+ 0 17		111	091	11 67	155	413	413
0 00	0 000	167	170	12 50	161	419	419
− 0 17	019	220	.245	13 33	166	424	424
− 0 33	026	250	278	14 17	.171	429	429
− 0 50	032	.272	291	15 00	176	434	434
− 0 67	037	286	303	15 83	181	.439	.439
− 0 83	041	298	.312	16 67	.186	444	444
− 1 00	046	308	322	17 50	190	449	.449
− 1 17	049	.318	.329	18 33	.194	454	.454
− 1 33	052	324	333	19 17	199	460	.460
− 1 50	056	330	.339	−20 00	0 203	0 465	0.465
− 1 67	0 059	0 335	0.343				

This function was computed numerically and is tabulated in Table 3. In Figure 3, our contrast transmission function is compared with the theoretical curve and with the function determined experimentally by Blackwell, Dewhirst, and Dollfus (1959) for their solar balloon telescope.

THE TRUE LIMB

To obtain the true limb intensity profile from the observed one, we use the apparatus function determined above and solve equation (2) by successive substitutions. That is, we first take some approximation to $T(x)$ and perform the summation indicated in equation (2). We then compare the result with the observed profile $O(x)$ and take the residuals as a correction to our assumed $T(x)$. We substitute this new $T(x)$ in equation (2) and continue in like manner until the residuals are as small as desired. This computation was carried out with the aid of an IBM 650 computer. The resulting true limb profile is shown in Figure 4 and tabulated in Table 2.

TABLE 3

CONTRAST TRANSMISSION FUNCTION

k	$T(k)$	k	$T(k)$	k	$T(k)$
0 0	1 000	5 6	0 485	11 2	0 196
0 4	0 949	6 0	462	11 6	179
0 8	0 896	6 4	.441	12 0	162
1 2	0 846	6 8	419	12 4	145
1 6	0 796	7 2	398	12 8	130
2 0	0 749	7 6	377	13 2	115
2 4	0 707	8 0	356	13 6	100
2 8	0.671	8 4	335	14 0	087
3 2	0 639	8 8	314	14 4	074
3 6	0 609	9 2	294	14 8	062
4 0	0 582	9 6	273	15 2	052
4 4	0 555	10 0	253	15 6	042
4 8	0 531	10 4	234	16 0	.033
5 2	0 507	10 8	0 215	16 4	0 026

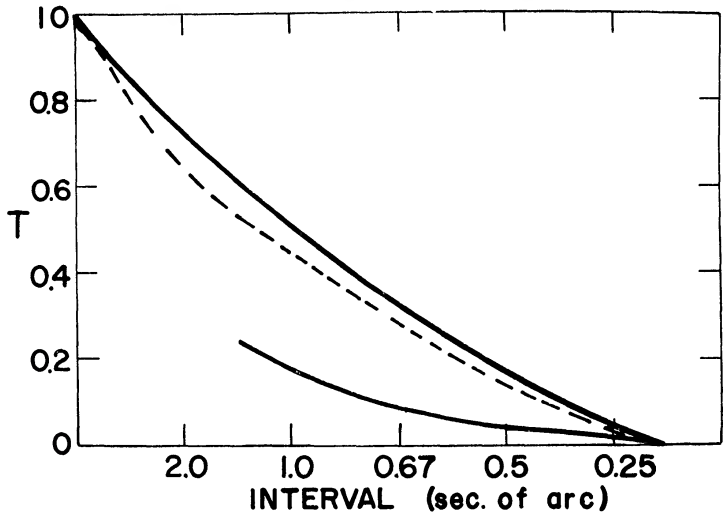

FIG. 3.—Contrast transmission function: theoretical curve (*heavy line*); the observed curve of Blackwell *et al.* (*light line*); Stratoscope curve (*dashed line*).

We also considered the possibility that the core of our apparatus function might better correspond to an effective aperture of only 10 inches instead of 12 inches. Using the fitting procedure described in the previous section, we constructed an apparatus function on this assumption, but we found that the true limb derived by using this function did not differ substantially from the other. Thus it appears that the wings of the apparatus function play an important role in the determination of the true limb, while the precise shape of the core does not.

As a check on our procedure, we compared the slope of our profile at the extreme limb with that obtained from eclipse measurements by Kristenson and Lindblad (Kristenson 1955). Our slope agrees with their determinations as well as they agree with each other. There is some indication that the value of the slope may vary with wave length; that is, our work is at a wave length intermediate to the above two, and our slope is also intermediate.

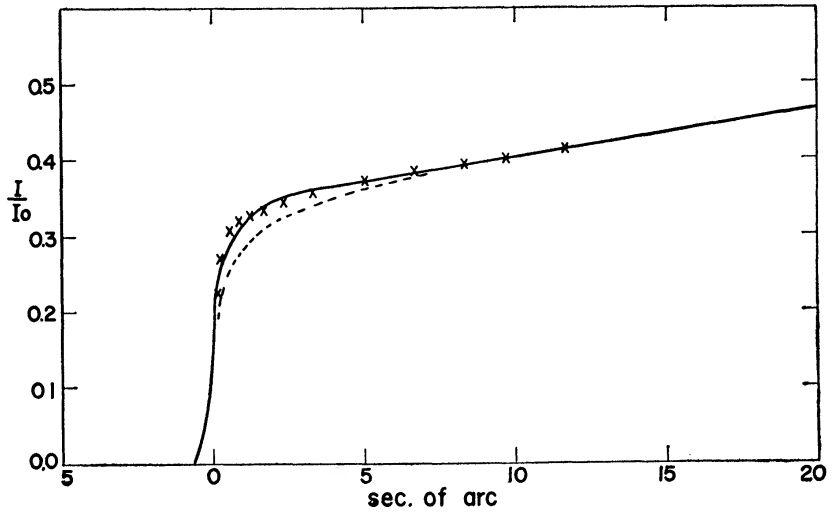

FIG. 4.—The solar limb intensity profile: true limb derived from 1959 Stratoscope photograph (*solid line*); Rogerson's true limb derived from 1957 Stratoscope photograph (*dashed line*); Dunn's limb profile (*crosses*).

The intensity measures described above were related to the intensity at the center of the solar disk with the aid of the Michigan limb-darkening data in the manner described by Rogerson (1959). However, in this case the measurements extend 20 seconds inside the limb, giving considerable overlap with the Michigan data, and the scaling can be done directly.

In Figure 4 the true limb thus derived is compared with that obtained previously by Rogerson (1959). The latter is seen to fall considerably lower. In the previous analysis it was impossible to determine the apparatus function experimentally because of the high threshold value of the emulsion. Therefore, the apparatus function was assumed to be the theoretical diffraction pattern for a 12-inch aperature. However, as shown above, the apparatus function does have extensive wings, much higher than the theoretical function. These wings have a very important effect in forming the observed limb profile, whereas the precise shape of the core does not. In addition, a comparison of the observations indicates that the wings of the apparatus function may have been even higher in the 1957 experiment. For these reasons, the assumption of a theoretical diffraction pattern led to a large undercorrection of the observed limb profile. The new determination, then, definitely supersedes the old one.

Also shown in Figure 4 are the observations of Dunn (1959), multiplied by a scale

factor of 0.783 for the sake of comparison. It is seen that the two determinations of the limb profile agree quite well, the difference being no more than that attributable to observational error.

It is a pleasure for the authors to acknowledge the many helpful discussions and suggestions provided by Dr. Martin Schwarzschild in the course of this work.

Project Stratoscope I is sponsored by the Office of Naval Research and the National Science Foundation.

REFERENCES

Bahng, J., and Schwarzschild, M. 1961, *Ap. J.*, **134**, 312.
Blackwell, D. E., Dewhirst, D. W., and Dollfus, A. 1959, *M.N.*, **119**, 98.
Bracewell, R. N., and Roberts, J. A. 1954, *Australian J. Phys.*, **7**, 615.
Danielson, R. E. 1961, *Ap. J.*, **134**, 275.
Dunn, R. B. 1959, *Ap. J.*, **130**, 977.
Elste, G. 1953, *Zs. f. Ap.*, **33**, 39.
Kristenson, H. 1951, *Stockholm Obs. Ann.*, **17**, 51.
———. 1960, *Ark. f. Astr.*, **2**, 324.
Rogerson, J. B., Jr., 1959, *Ap. J.*, **130**, 985.
———. 1961, *Ap. J.*, **134**, 331.

FIG. 1.—Photograph of facular region with photometered faculae marked by arrows. Scale: 1 cm = 6.4 seconds of arc.